Decadal Sea Level Changes in the 50-Year GECCO Ocean Synthesis

Armin Köhl, Theodoros Yemenis, and Detlef Stammer

Institut für Meereskunde, ZMAW, Universität Hamburg, Germany

Summary

The consortium for Estimating the Circulation and Climate of the Ocean (ECCO) has demonstrated the feasibility and skill of global estimates of the full three-dimensional, time-varying oceanic state over the period 1992-2002 (Köhl et al., 2006b). Parallelling the 50 year NCEP/NCAR reanalysis an estimation of the ocean circulation and its changes was obtained over the period 1952-2002 (Köhl et al., 2006a) and is being analyzed with respect to its decadal and longer term changes in sea level. The synthesis combines most of the data set available during this period with the MIT/ECCO ocean circulation model using its adjoint over the entire period. Regional changes in sea level over the last decade are described and compared with results obtained from TOPEX and from an earlier shorter optimization. The trends over the last decade are compared with those obtained over the pre-Topex period.

Optimization

The approach is identical to the 11 year ECCO estimation in which initial temperature and salinity conditions as well as the time-dependent surface fluxes of momentum, heat and freshwater are adjusted by the adjoint method in order to bring a global 1 degree model into agreement with observations. Before 1992 the state is mainly constrained by an extensive data base of sub-surface XBT and MBT measurements whereas only after 1992 the same data rich data base is available as for the 11 year estimation. We show results of iteration 23.

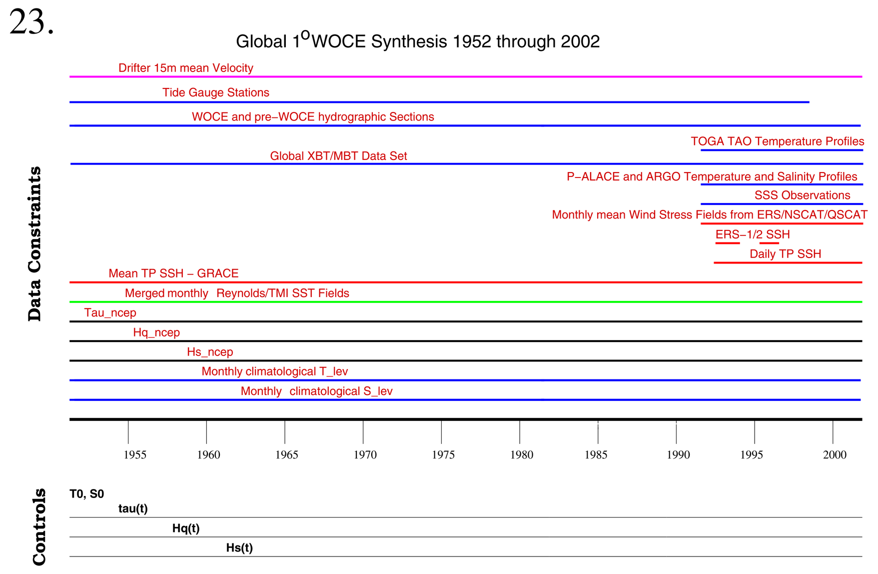

Fig. 1: Schematic of the optimization. The upper part shows the data constraints imposed on the model. The lines indicate times when data is available, mean or climatological data is shown as being available throughout the whole period. The lower part summarizes the control parameters that were changed during the optimization.

SSH and steric changes

For the analysis of SSH trends with a model that uses the Boussinesq approximation one has to keep in mind that this model conserves volume and that the globally averaged SSH is not permitted to change with time. We here concentrate therefore on regional SSH changes only as well as the steric components.

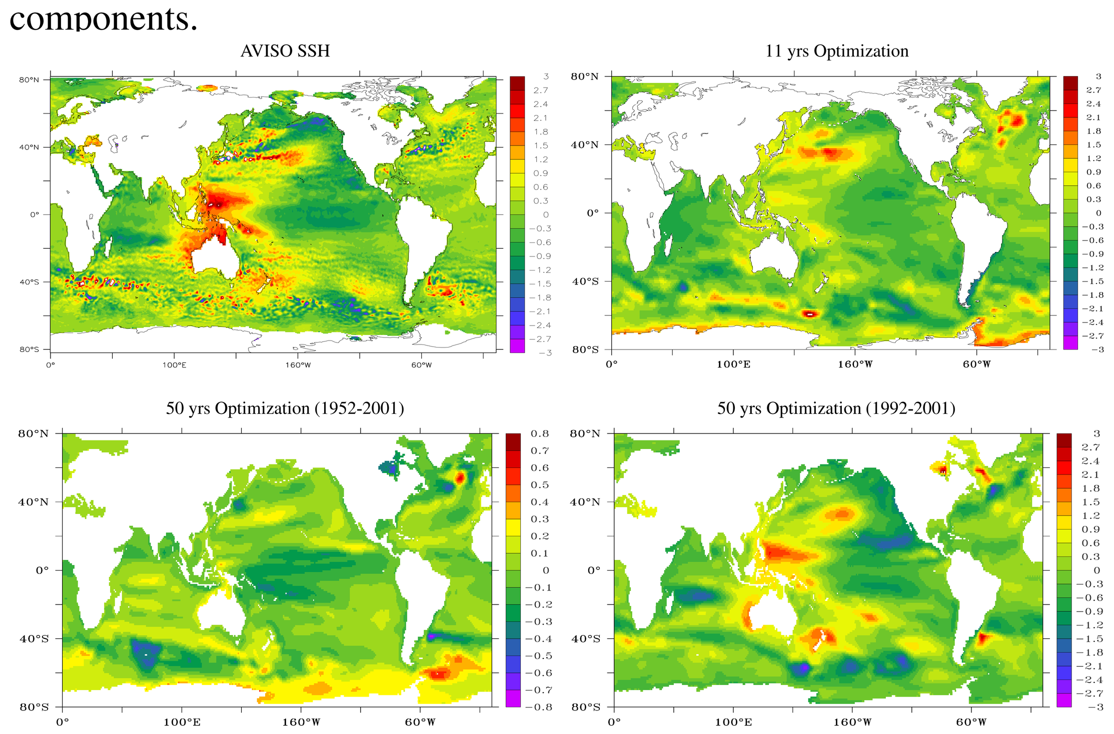

Fig. 2: SSH trends in cm/year from altimeter data and ocean state estimations. Top row: mapped AVISO SSH (left) and SSH form the 11 years optimization (right). Bottom row: SSH trend from the 50 years optmization for the total period 1952-2001 (left) and the last decade (1992-2001) (right).

Amplitude and patterns (Fig. 2 lower right) of the trend match the observed changes during the last decade which greatly differs from the trend over the complete 50 years. At large, both patterns of the trends seem to opposes each other. Patterns of the linear drift of the SSH shows the deceleration of the ACC (about 20 Sv over 50 years) and intensification of the subtropical and subpolar gyres (Fig. 2 lower left). In comparison to the previous 11 years optmization, the estimation over the 50 years clearly shows a considerable improvement of simulating the observed SSH trend during the last decade.

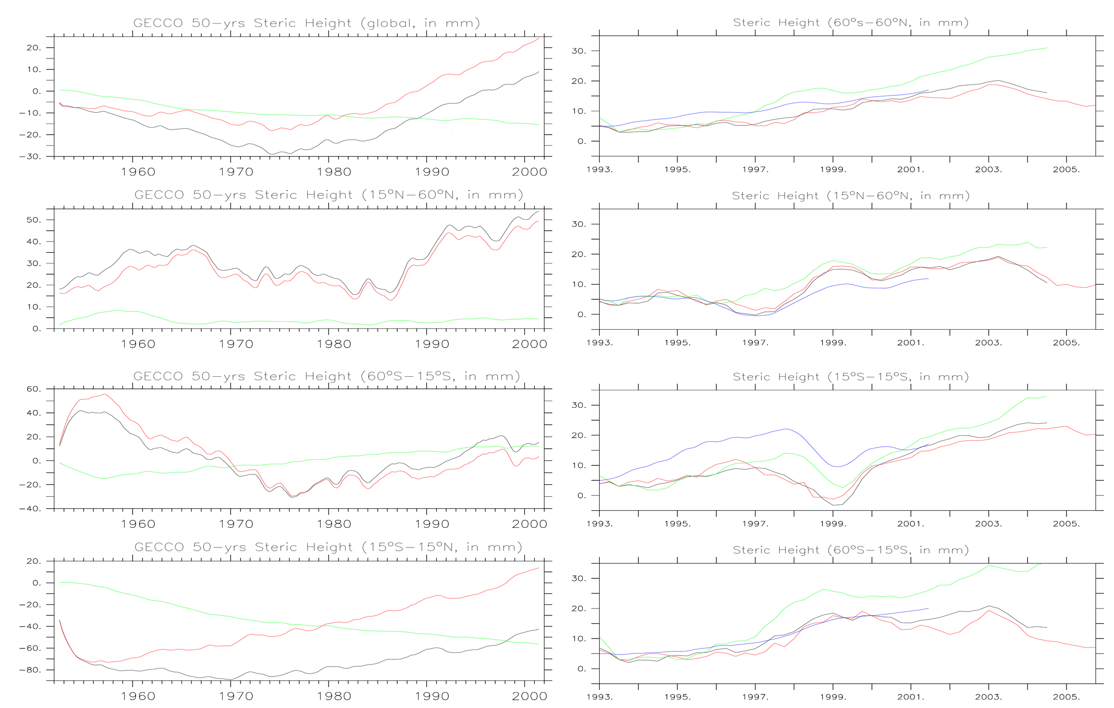

Fig. 3: (Right) Total sea level (black, source:AVISO) and thermosteric (0 - 750 m) sea level estimated from in situ data only (red) and using the altimeter/thermosteric height correlation as a first guess (green) for objective mapping of the in situ data. (From Willis et al, 2004 and Lyman et al, 2006) together with the thermosteric sea level form the GECCO 50-year ocean synthesi. (Left) Total steric (black), thermosteric (red) sea level and halosteric component (green) from the GECCO estimate.

Fig. 3 shows timeseries of global as well as regional trends of the steric components, split up into thermo- and halosteric parts, over the 50 years. The thermosteric component shows in general good agreement with the estimate of Willis et al. (2004) and Lyman et al. (2006). SSH trends are not shown from our estimate. The trend of the thermosteric part amounts to 2 mm per year over the last decade which is close to other recent estimates.

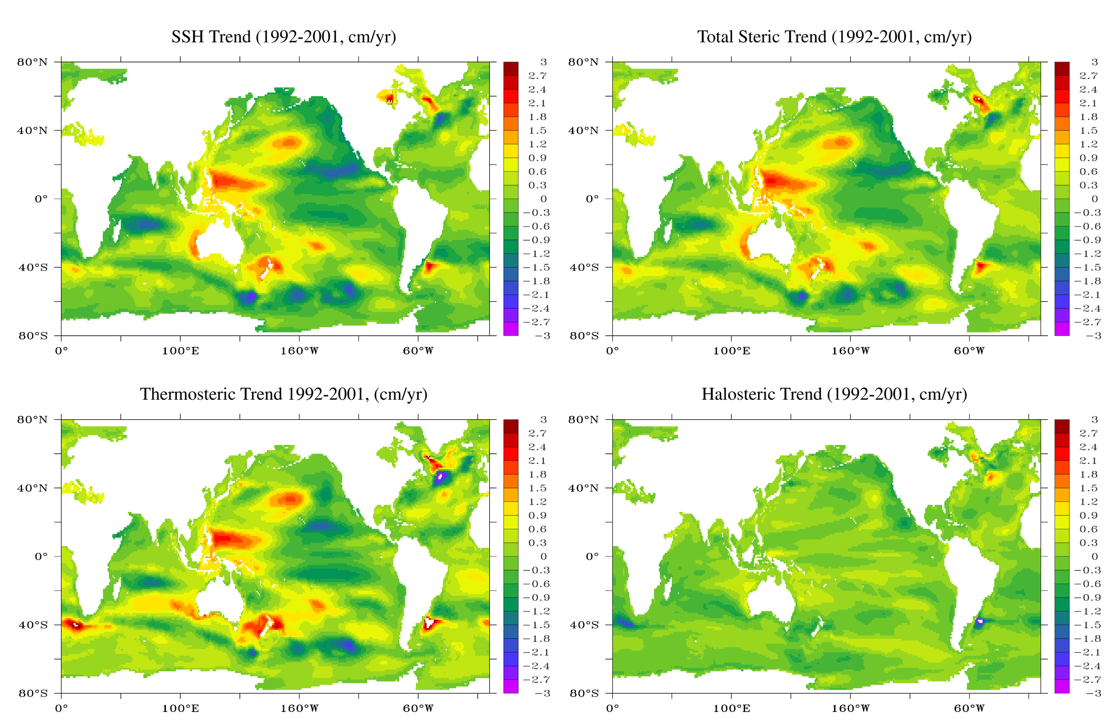

Fig. 4: Top row: Model SSH trend (left) and steric SSH trend (right) estimated over the last decade of the 50 years period 1952 through 2001 from the model potential density field. Bottom row: Corresponding thermo-steric (left) and halo-steric (right) sea level change All fields are in cm/yr.

The SSH trend during the last decade is well constrained by direct altimetric SSH measurements. The steric component explains most of the trend that is mainly due do the thermosteric part. The latter is partly reduced by the halosteric contribution.

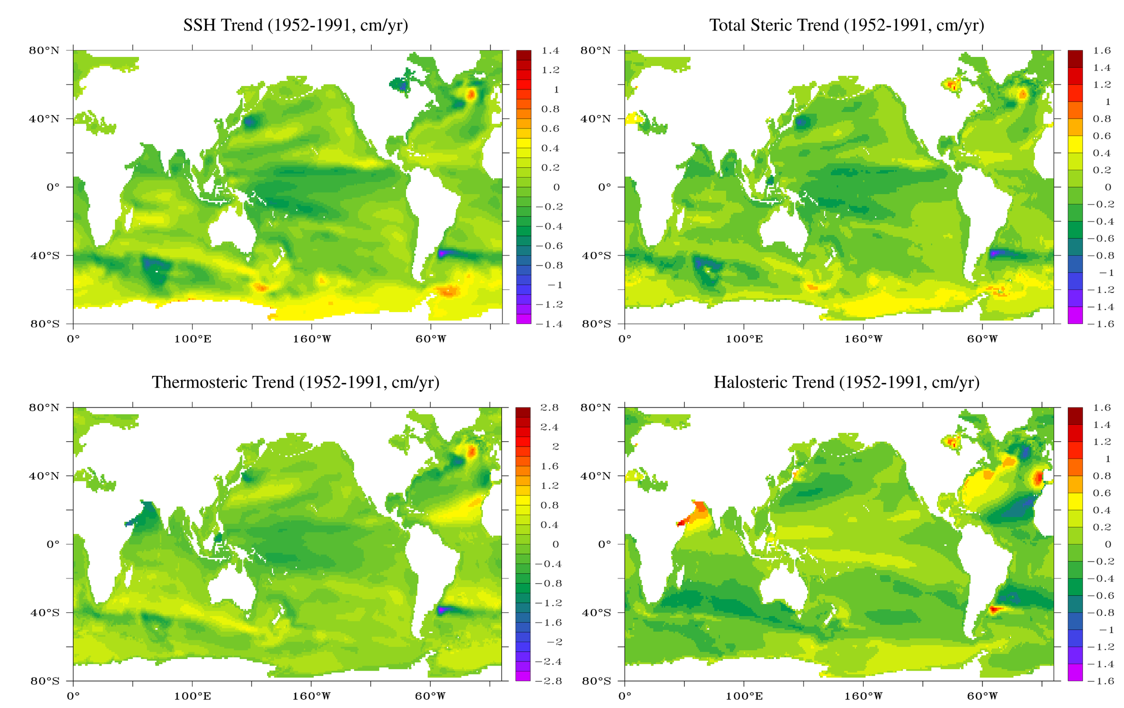

Fig. 5: Top row: Model SSH trend (left) and steric SSH trend (right) estimated over the first 4 decades of the 50 years period 1952 through 2001 which are not constrained by direct altimetric SSH observations. Bottom row: Corresponding thermo-steric (left) and halo-steric (right) sea level change All fields are in cm/yr.

The SSH trend during the first 4 decades is in general only about one third of the trend of the last decade. The steric component explains as before most of the trend. For most regions the trend is reversed in comparison to the last decade. The contribution of the thermosteric part, however, is now strongly reduced by the halosteric component which results in a total steric component that is considerably smaller than the thermosteric part.

Mechanisms

The trend of the barotropic stream function (1cm $\sim$ 1Sv, typically) corresponds well with the SSH trend (compare Fig. 6 and Fig.4). Although patterns of the trend of the Sverdrup transports correspond reasonably well with the trend of the stream function, changes of wind stress curl are only able to explain about 10% of the trend.

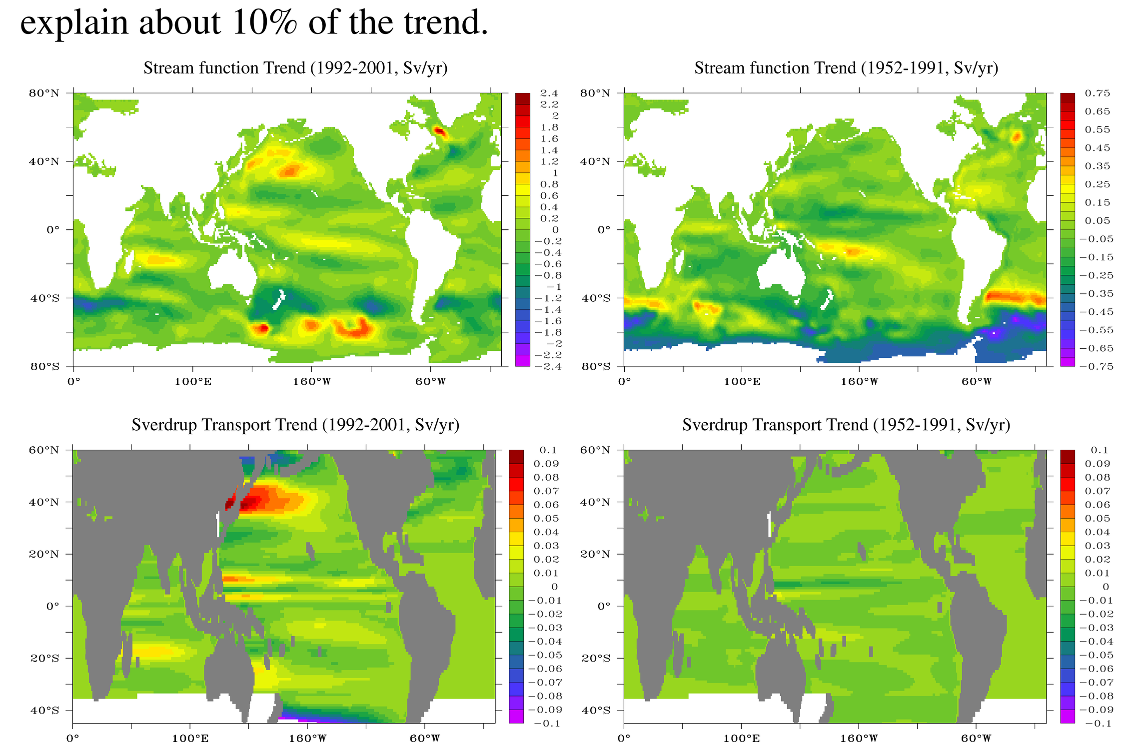

Fig. 6: Top row: Trends of the barotropic stream function for the last decade (1992-2001, left) and first 4 decades (1952-1991, right) of the 50 years optimization in Sv/yr. Bottom row: Trends of the Sverdrup transports from the corresponding wind stress curl estimation for the last decade (1992-2001, left) and first 4 decades (1952-1991, right) of the 50 years optimization in Sv/yr.

Long term changes may be explained by a relaxation process from an anomalous year (e.g. and El Nino year) towards the equilibrium state. Comparing Fig. 7 with Fig. 5 and 4, respectively, reveals that much of the regional trends (about 2 cm/year for the period 1992-2001) can be explained by an anomalous year.

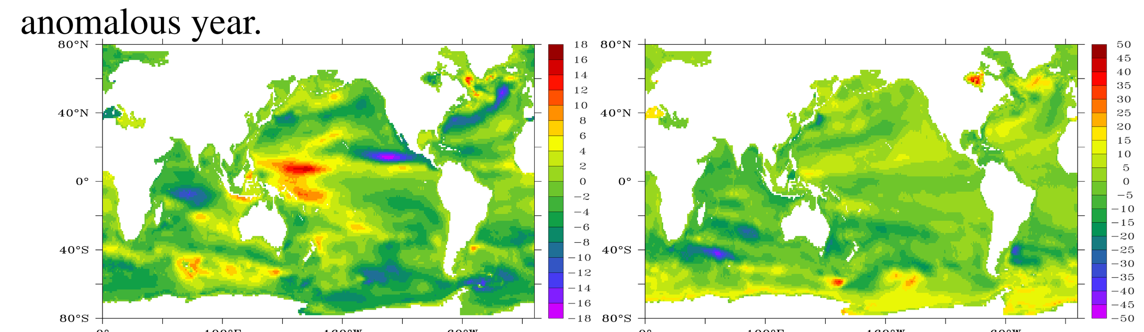

Fig. 7: Steric anomaly of year 1992 (mean mid 1991- mid 1992) (left) and of year 1952 (right) with respect to the 50 years mean multiplied by -1. Units are cm

Figs. 8 shows estimated heat content changes as function of time. Also shown are respective estimates inferred from Levitus et al. (2004). The total heat content changes show a trend to lower values during the first 15 years. The overall changes over the full 50 years is slightly smaller than those reported by Levitus et al. (2004) but considerably larger over the last 30 years. A further difference is noticeable in the upper 300m for which no change is observed over the 50 years.

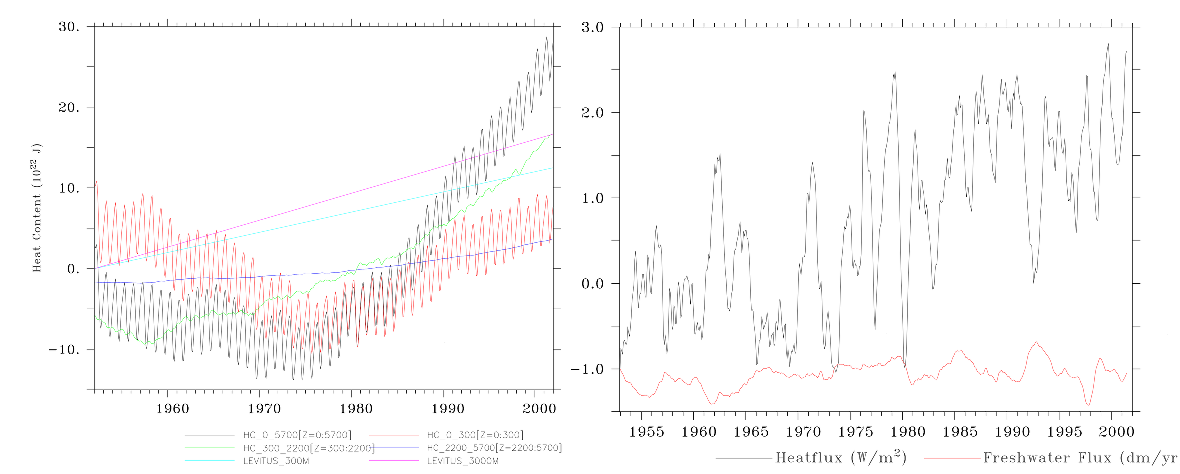

Fig. 8: (Left) Time series of the global heat content (black) plotted together with those computed separately over the top 510m (red), from 510m to 2200m (green), and from 2200m to the bottom (blue). Also shown is an estimate of global heat content increase as it would follow from the linear trend of Levitus et al. (2004) over the top 300m (cyan) and the top 3000m (magenta). A temporal mean was removed from all curves. (Right) Time series of the globally averaged heat and freshwater flux in W/m^2.

Changes of the globally averaged heatflux are consistent with the warming trend. Since the mid 70ies the global bias of the heatflux increased from values around zero to values between 1 and 2 W/m^2 during the nineties. NCEP values, in comparison, range from -6 W/m^2 at the begining of the 60ies to +6 W/m^2 in the mid 80ies. The freshwater flux is with 10 dm/yr on the global mean unrealisticly high and not much different to the NCEP value of 7 dm/yr which indicates that the amount of available salinity data together with the low sensitivity to freshwater flux changes does not permit the estimation of the global mean freshwater flux.

Conclusion

Results from the optimization demonstrate that longterm state estimation efforts are necessary for simulating present day SSH changes.

- The 50yrs optmization shows better skills in simulating the last decade of SSH changes than the previous 11 years optimization of only the last decade.
- Halosteric and thermosteric changes in general oppose each other. A general heating is accompanied with a general freshwater loss.
- Heating trends are observable in the southern hemisphere from the beginning of the estimation in the mid 50ies but are visible in the northern hemisphere only since the beginning of the 80ies.
- The tropics show a cooling until mid 70ies and a warming thereafter.
- The dominance of linear trends is observable since the mid 70ies.
- Regional trends observed turing the TOPEX/POSEIDON period are largely explained by anomalies during 1992.

References

Köhl, A., D. Dommenget, K. Ueyoshi, and D. Stammer, 2006a: The global ECCO 1952 to 2001 ocean synthesis, *ECCO Report No.40*, See also http://www.ecco–group.org/reports.html.

Köhl, A., D. Stammer, and B. Cornuelle, 2006b: Interannual to decadal changes in the ECCO global WOCE synthesis, *J. Phys. Oceanogr.*, in press.

Levitus, S., J. Antonov, and T. Boyer, 2004: Warming of the world ocean, 1955-2003, *Geophys. Res. Lett.*, **32**, doi:10.1029/2004GL021791.